Modification of Quark-Gluon Distributions in Nuclei by Correlated Nucleon Pairs

A. W. Denniston,[1,*] T. Ježo,[2,†] A. Kusina,[3] N. Derakhshanian,[3] P. Duwentäster,[2,4,5] O. Hen,[1] C. Keppel,[6] M. Klasen,[2,7] K. Kovařík,[2] J. G. Morfín,[8] K. F. Muzakka,[2,9] F. I. Olness,[10] E. Piasetzky,[11] P. Risse,[2] R. Ruiz,[3] I. Schienbein,[12] and J. Y. Yu.[12]

[1]*Massachusetts Institute of Technology, Cambridge, Massachusetts 02139, USA*
[2]*Institut für Theoretische Physik, Universität Münster, Wilhelm-Klemm-Straße 9, D-48149 Münster, Germany*
[3]*Institute of Nuclear Physics Polish Academy of Sciences, PL-31342 Krakow, Poland*
[4]*University of Jyväskylä, Department of Physics, P.O. Box 35, FI-40014 University of Jyväskylä, Finland*
[5]*Helsinki Institute of Physics, P.O. Box 64, FI-00014 University of Helsinki, Finland*
[6]*Jefferson Lab, Newport News, Virginia 23606, USA*
[7]*School of Physics, The University of New South Wales, Sydney NSW 2052, Australia*
[8]*Fermi National Accelerator Laboratory, Batavia, Illinois 60510, USA*
[9]*Institut für Energie- und Klimaforschung, Forschungszentrum Jülich GmbH, 52425 Jülich, Germany*
[10]*Department of Physics, Southern Methodist University, Dallas, Texas 75275-0175, USA*
[11]*School of Physics and Astronomy, Tel Aviv University, Tel Aviv 6997845, Israel*
[12]*Laboratoire de Physique Subatomique et de Cosmologie, Université Grenoble-Alpes, CNRS/IN2P3, 53 avenue des Martyrs, 38026 Grenoble, France*

(Received 15 January 2024; revised 19 April 2024; accepted 7 August 2024; published 11 October 2024)

We extend the QCD Parton Model analysis using a factorized nuclear structure model incorporating individual nucleons and pairs of correlated nucleons. Our analysis of high-energy data from lepton deep-inelastic scattering, Drell-Yan, and W and Z boson production simultaneously extracts the universal effective distribution of quarks and gluons inside correlated nucleon pairs, and their nucleus-specific fractions. Such successful extraction of these universal distributions marks a significant advance in our understanding of nuclear structure properties connecting nucleon- and parton-level quantities.

DOI: 10.1103/PhysRevLett.133.152502

Introduction—Subatomic systems, such as nucleons and atomic nuclei, and dense astrophysical matter, derive their properties from the many-body interactions between their constituent quarks and gluons, which are described by the theory of quantum chromodynamics (QCD). The strongly coupled nature of QCD links the momentum distribution of quarks and gluons in these systems to their structure and emergent properties, such as mass and spin [1]. Therefore, it is crucial to understand the momentum distribution of quarks and gluons in nucleons and nuclei.

By analyzing high-energy collisions between leptons, nucleons, and nuclei, using a well-established QCD factorization formalism [2–4], parton distribution functions (PDFs) can be extracted for both nucleons and nuclei. These PDFs describe the fraction of the total system momentum carried by different flavored quarks and gluons [5–7]. The nuclear PDFs (nPDFs) are observed to differ from the simple sum of their free-proton and free-neutron PDFs, indicating a measurable role of nuclear dynamics that remains to be understood [8–13].

Compared to the nucleon PDFs, the nuclear PDFs are impacted by various nuclear effects due to the spatial distribution of nucleons in the nucleus (shadowing and antishadowing), their motion (Fermi motion), and strong interactions between nucleons affecting their internal parton structure [14,15]. The standard global analyses (such as nCTEQ [8,12,16–19], EPPS [9,20], nNNPDF [11,21,22], TUJU [10,23], DSSZ [24], Khanpour *et al.* [25,26]) extract parton densities inside the *full nucleus* using experimental data.

Here, we propose to use state-of-the-art knowledge of nuclear theory to guide the development of nuclear PDFs:

Nuclei are commonly described as a group of independent nucleons moving within an effective average mean field that leads to the population of atomlike nuclear shells [27]. In this picture, nuclear effects are modeled in the nPDFs by consistently modifying all nucleons under the effective influence of the nuclear mean field. It is important to note that this does not allow for a meaningful interpretation in terms of modified parton densities inside bound single nucleon states since they incorporate effects from many nucleon states present in the data.

*Contact author: awild@mit.edu
†Contact author: tomas.jezo@uni-muenster.de

Nuclear structure studies show that the formation of short-lived excitations, caused by strongly interacting short-range correlated (SRC) nucleon pairs [28–31] are significant. While the abundance of SRC pairs differs among nuclei, they are predominantly proton-neutron pairs [28,32–37] and have the same behavior in all nuclei [29,30,38–40]. Consequently, SRC pairs have universal properties across nuclei and typical separation energies of 15%–30% of the nucleon mass, which is significantly higher than that of mean-field states [39–42]. The large energies and significant spatial overlaps of SRC pairs motivated various studies of the relation between SRC pairs and bound-nucleon structure [29].

This analysis studies nPDFs based on our understanding of high-resolution nuclear structure with SRCs. It allows for the first time to split the partonic structure inside nuclei into mean-field and SRC contributions and to extract information on nuclear structure from an analysis of the partonic content of nuclei. We try to take a model-agnostic approach by focusing on the broad-scale features common to modern high-resolution nuclear structure models, minimizing dependence on specific model details.

Short-range nuclear structure—The fundamental quantity of nuclear structure that is relevant for our study is the nuclear spectral function $S_A(k,E)$ that defines the probability of finding a nucleon with momentum k and separation energy E in a nucleus with mass number A. We use a normalization convention of $\int S_A(k,E)k^2 dkdE \equiv 1$.

Direct many-body calculations of $S_A(k,E)$ are computationally unfeasible for $A > 3$ nuclei. Therefore, we employ an established approximation where the spectral function is divided into two parts [30],

$$S_A(k,E) = S_A^{\mathrm{MF}}(k,E) + S_A^{\mathrm{SRC}}(k,E), \tag{1}$$

with $S_A^{\mathrm{MF}}(k,E)$ representing the single nucleons in a mean field (MF), and $S_A^{\mathrm{SRC}}(k,E)$ representing the spectral function of nucleons in SRC pairs.

The separation presented in Eq. (1) is rooted in the vastly different energy scales associated with the single-nucleon mean-field potential and the interaction energy inside SRC pairs. While mean-field nucleons have momenta and energy below nuclear Fermi momentum ($k_F \sim 250$ MeV/c) and Fermi energy $E_F \sim 35$ MeV, the strong pairwise interaction energy inside SRC pairs leads to relative momenta of 300–800 MeV/c and separation energies of 150–400 MeV [39–42].

The high-energy scale associated with interactions in SRC pairs leads to a further factorization of their spectral function into a universal (nucleus independent) pair spectral function distribution, scaled by a (nucleus dependent) pair abundance factor [41],

$$S_A^{\mathrm{SRC}}(k,E) \approx \frac{Z}{A} C_p^A \times S_p^{\mathrm{SRC}}(k,E) + \frac{N}{A} C_n^A \times S_n^{\mathrm{SRC}}(k,E). \tag{2}$$

In the above approximation, we do consider all possible (pn), (pp), and (nn) nucleon-nucleon pairs by introducing effective coefficients, $C_{p(n)}^A$, that sum the number of (pn), (pp) and (nn), (np) pairs, respectively.

Here, C_N^A $(N = p,\ n)$ are nucleus-dependent constants that "count" the fraction of nucleons in SRC pairs, and $S_N^{\mathrm{SRC}}(k,E)$ are universal (nucleus-independent) pair distributions that are dominated by the strong nucleon-nucleon interaction at short distance. Z and N are the total number of protons and neutrons in the nucleus $(Z + N = A)$. The universal pair spectral functions follow normalization conventions of $\int S_N^{\mathrm{SRC}}(k,E)k^2 dkdE \equiv 1$ $(N = p,\ n)$ and therefore $\int S_A^{\mathrm{MF}}(k,E)k^2 dkdE = 1 - (ZC_p^A + NC_n^A)/A$.

Combining Eqs. (1) and (2) we obtain

$$S_A(k,E) \approx S_A^{\mathrm{MF}}(k,E) + \frac{Z}{A} C_p^A \times S_p^{\mathrm{SRC}}(k,E) + \frac{N}{A} C_n^A \times S_n^{\mathrm{SRC}}(k,E), \tag{3}$$

where we emphasize that the mean-field term $S_A^{\mathrm{MF}}(k,E)$ captures low-energy, single nucleon dynamics and the SRC terms $C_N^A \times S_N^{\mathrm{SRC}}(k,E)$ captures universal high-energy nucleon-pair dynamics.

We note that the approximation presented in Eq. (3) enjoys significant support [36,39,41,43–46] by recent analyses of *ab initio* many-body nuclear structure calculations and high-energy electro-induced nucleon knockout measurements. Furthermore, Eq. (1) can in principle be extended to also include three-nucleon correlation effects that are neglected in the context of this Letter.

SRC motivated nuclear-PDFs—nPDFs are defined within perturbative QCD using the framework of collinear factorization [3,47]. This framework allows the computation of cross sections, $d\sigma_{AB\to X}$, for scattering of particles A, B into final state X as convolutions of perturbatively calculable parton-level short-distance cross sections, $d\hat{\sigma}_{ij\to X}$, and nonperturbative PDFs, $f_{i(j)}$, where i and j sum over the partonic content of hadrons A and B, respectively.

Introducing these nuclear quark and gluon distributions to the nuclear structure model of Eqs. (1) and (2) leads to an nPDF parametrization that is composed of a linear combination of free-nucleon PDFs (representing the quasifree nucleons), and SRC PDFs that describe the universal quark and gluon distributions inside an SRC pair,

$$f_i^A(x,Q) = \frac{Z}{A}[(1 - C_p^A) \times f_i^p(x,Q) + C_p^A \times f_i^{\mathrm{SRC}p}(x,Q)] + \frac{N}{A}[(1 - C_n^A) \times f_i^n(x,Q) + C_n^A \times f_i^{\mathrm{SRC}n}(x,Q)]. \tag{4}$$

Here, $f_i^A(x,Q)$ is the nPDF of parton type i (gluon or quark flavors) in a nucleus with mass number A, carrying momentum fraction x at energy scale Q. $f_i^N(x,Q)$ and $f_i^{\mathrm{SRC}N}(x,Q)$ are the PDFs of the free nucleon and of the modified nucleon in an SRC pair, respectively. Here, we implicitly assume that $f_i^{\mathrm{SRC}N}(x,Q)$ can be defined via a collinear factorization framework, and that the proton and neutron distributions are related by isospin. Therefore, we apply the tools from perturbative QCD used for free-nucleon PDFs to arrive at the physical predictions (e.g., Dokshitzer-Gribov-Lipatov-Altarelli-Parisi evolution).

A key feature of this framework is that the nuclear structure dependence is fully encapsulated in the fraction of nucleons in SRC pairs C_N^A.

As we do not separate the individual effects of proton-proton, neutron-neutron, and proton-neutron SRCs, Eq. (4) relates the modified structure of an average nucleon in an SRC pair, independent of its pair configuration.

We keep a model-independent approach as to the number of SRC pairs and their isospin structure. In fact, these nuclear structure parameters will be independently determined in our nPDF analysis for the first time (cf. Fig. 1), and tested for consistency with independent results from specific nuclear structure studies.

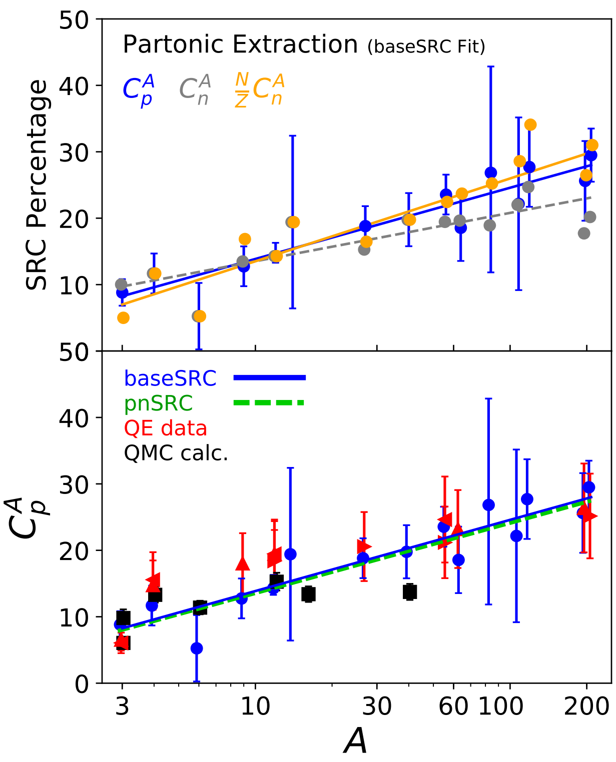

FIG. 1. (a) Comparison of nuclear structure parameters C_p^A, C_n^A, and $(N/Z)C_n^A$ values for the baseSRC fit. The solid lines represent logarithmic fits to the corresponding quantities. We show uncertainties only for the C_p^A, but errors for other quantities are of similar size. (b) Comparison of C_p^A values for the baseSRC fit and the SRC abundances extracted from quasielastic (QE) [48–50] data and quantum Monte Carlo (QMC) [46] nuclear calculations. The logarithmic fits for baseSRC and pnSRC are also shown.

We further note that Eq. (4) represents a natural evolution of previous studies that (i) observed a linear correlation between measured SRC abundances and the modified structure of bound nucleons in the valence region (i.e., at high fractional momentum $x \sim 0.3$–0.7), known as the EMC effect [51–53], and (ii) showed that this correlation can result from a universal modification of the valence region structure function of nucleons in proton-neutron SRC pairs [50]. These studies were limited to the nucleon valence region ($x \sim 0.3$–0.7) and using lepton-nucleus deep inelastic scattering (DIS) data with specific nuclear structure input for SRC abundances [50,54]. As detailed below, here we study the fundamental nPDFs, extend the analysis to the full x range of 10^{-3} to 0.8, use a comprehensive dataset on the parton structure of nuclei, and do not impose external inputs for nuclear structure parameters C_N^A. The latter is especially important as the independent extraction of C_N^A allows us to compare with known measured and calculated nuclear structure values to support, or challenge, the physical validity and interpretation of Eq. (4).

As the DIS coherence length scales as $1/x$, it is more natural to associate higher-x phenomena with short-range nuclear physics than very low-x ($x \sim 10^{-2} - 10^{-3}$) phenomena. Low-x reactions are sensitive to the number of nucleons the virtual photon propagates through, given by the nuclear thickness function [14]

$$T^{(2)}(b) = \int dz_1 \int dz_2 \rho^{(2)}(b_1 = b, z_1; b_2 = b, z_2), \qquad (5)$$

where $\rho^{(2)}$ is the two-nucleon density defining the probability for finding two nucleons with transverse and longitudinal positions b and z. For mean-field models, we can assume $\rho^{(2)}$ approximately factorizes into $\sim\rho(b_1, z_1)\rho(b_2, z_2)$. Studies show the SRC pairs significantly impact the two-nucleon density leading to a typical correction of [55,56]

$$\rho^{(2)}(b_1, z_1; b_2, z_2) \approx \rho(b_1, z_1)\rho(b_2, z_2)\{1 + C(|z_1 - z_2|)\}. \qquad (6)$$

Here, the correlation function $C(|z_1 - z_2|)$ is sensitive to the number of nucleons in SRC pairs (i.e., C_N^A). Therefore, $\rho^{(2)}$ modifies the nuclear thickness function, which will impact the low-x region. This does not mean to imply that the measured behavior at low-x stems only from the modification of the structure of nucleons in SRC pairs, but it can potentially depend on the SRC-induced correlation. This requires further investigation with additional low-x data.

Analysis and results—The analysis utilized the full set of available world data on nuclear lepton DIS, Drell-Yan processes, and W and Z boson production (see the Supplemental Material [57] for dataset details). The corresponding theory predictions were obtained in collinear factorization with the parton-level cross-sections calculated at the next-to-leading order of QCD. The DIS data primarily constrain the u and d quark and antiquark distributions, whereas the W and Z boson production data from LHC proton-lead collisions also constrain strange quark and gluon distributions down to lower momentum fractions of $x \sim 10^{-3}$.

Energy scale dependence is accounted for using the Dokshitzer-Gribov-Lipatov-Altarelli-Parisi evolution equation, which also helps constrain the gluon distribution through the Q dependence of DIS data. Parton number and momentum sum rules are ensured to be separately satisfied for $f_i^{p(n)}(x, Q)$ and $f_i^{\mathrm{SRC}p(n)}(x, Q)$, and are therefore also satisfied for their linear combination in Eq. (4) independently of the values of C_p^A and C_n^A. (Note that the sum rules for the free-nucleon distributions are satisfied by construction. This is ensured by relying on the free-nucleon PDFs determined in a dedicated fit [66].)

The free-nucleon PDFs $f_i^{p(n)}(x, Q)$ are fixed to the distributions determined in Ref. [8] via global analysis of nucleon structure observables. The SRC nucleon PDFs $f_i^{\mathrm{SRC}p(n)}(x, Q)$ use the same functional form as $f_i^{p(n)}(x, Q)$ with 21 shape parameters that are fit herein. We perform two independent analyses where (i) C_p^A and C_n^A are allowed to vary freely, and (ii) where we assume proton-neutron SRC dominance, i.e., $C_p^A = (N/Z) \times C_n^A \equiv C^A$. We refer to these fits as the baseSRC and pnSRC fits, respectively. For comparison, we also repeated the TRADITIONAL (mean-field-like) analysis of Ref. [12] using the same dataset used herein, which we refer to as the "TRADITIONAL" fit.

The resulting fit quality in terms of χ^2 for each SRC fit and for the TRADITIONAL fit are listed in Table I for each data type separately, and for all data combined. As can be seen, the SRC fit using Eq. (4) results in overall $\chi^2_{\mathrm{tot}}/N_{\mathrm{d.o.f.}}$ values appreciably better than for the TRADITIONAL fit. This takes into account the additional SRC ($C_{p,n}^A$) parameters. At the level of the total χ^2 we obtain a reduction of 108 and 58 points for the baseSRC and the pnSRC fits, respectively. We find that the nPDFs for the TRADITIONAL and SRC fits are in general agreement within uncertainties. All data are well reproduced for the full range of the data, corresponding to an x range of about 10^{-3} to 0.75.

Figure 1 shows the extracted C_p^A and C_n^A coefficients as determined by the global baseSRC. The coefficients show logarithmic growth with the nuclear mass number A, starting from ∼5% for helium-3 and reaching ∼20% for lead. As shown in Fig. 1(b), the baseSRC and pnSRC fits give similar results with the baseSRC fit preferring a similar number of SRC protons and neutrons, even for heavy neutron-rich nuclei. This dynamics is consistent with the observation of pn dominance, previously determined from nuclear structure studies [28,32]. Therefore, the baseSRC and pnSRC consistency is a first indication of consistency between quark-gluon level analysis and nuclear structure studies.

TABLE I. The partial χ^2/N_{data} values for the data subsets; the number of data points (N_{data}) for each process are listed in the bottom row. The TRADITIONAL fit has 19 shape and $3W$ and Z boson (W/Z) normalization parameters. The baseSRC and pnSRC fits have 21 shape, $3W/Z$ normalization, and 30 and 19 SRC parameters ($C_A^{p,n}$), respectively. In total, there are 1684 data points after cuts. Note the last column ($\chi^2_{\mathrm{tot}}/N_{\mathrm{d.o.f.}}$) fully takes into account the number of fit parameters.

χ^2/N_{data}	DIS	DY	W/Z	JLab	χ^2_{tot}	$\chi^2_{\mathrm{tot}}/N_{\mathrm{d.o.f.}}$
TRADITIONAL	0.85	0.97	0.88	0.72	1408	0.85
baseSRC	0.84	0.75	1.11	0.41	1300	0.80
pnSRC	0.85	0.84	1.14	0.49	1350	0.82
N_{data}	1136	92	120	336	1684	

Focusing on the lower panel, Fig. 1 also shows the extracted C_p^A coefficients are consistent with previous, independent extractions from both nuclear structure calculations [46] and quasielastic electron scattering measurements [48–50]. As the nuclear structure calculations assume pointlike nucleons, and the measurements are done at energies that only probe nucleons (and not their substructure), they are both insensitive to the nucleon nPDFs.

Therefore, we report here the first direct extraction of nuclear structure information from parton-level observables in an nPDF data analysis that is fully consistent with independent nuclear structure extractions.

Finally, looking at the nucleon structure itself, Fig. 2 shows the ratios of rescaled structure functions F_2^A/A, compared to the F_2 isoscalar (i.e., $(F_2^p + F_2^n)/2$) for the TRADITIONAL fit. We also compute the F_2 structure function ratio for nucleons in SRC pairs relative to F_2 isoscalar; results shown are obtained from the baseSRC fit (blue curve). Direct measurements of the ratio F_2^A/A to F_2 isoscalar exist for the low A deuteron and triton measurements [67,68] that are not included in the present analysis; extending the current analysis to lighter nuclei, including the mirror nuclei ^{3}H and ^{3}He, are planned for future study.

As can be seen in Fig. 2, the SRC and TRADITIONAL curves both result in qualitatively similar deviations from the free-nucleon structure, with the SRC showing significantly larger modification than even lead (Pb) in the TRADITIONAL case. This is expected as the SRC curve corresponds only to the one component of full distribution [c.f. Eq. (4)], which is responsible for the whole nuclear modification. The amount by which the SRC modification is larger than the TRADITIONAL case, however, varies significantly with x. At very low x, below $2-3\times10^{-2}$, we observe only a slightly increased suppression for the SRC case. At intermediate x of $2-3\times10^{-2}$ to 2×10^{-1} we observe a more pronounced difference between the SRC

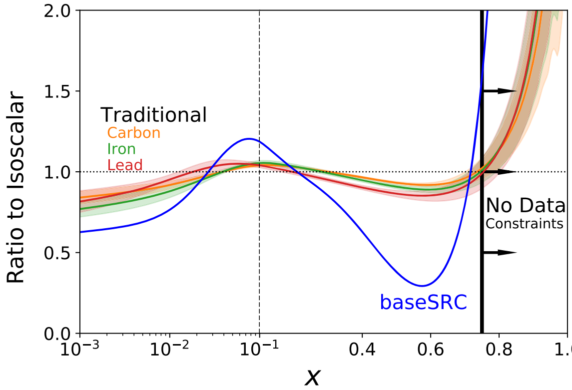

FIG. 2. The ratio of the rescaled structure function F_2^A/A to the isoscalar combination $(F_2^p + F_2^n)/2$, computed for the TRADITIONAL PDFs for carbon, iron, and lead. Separately, we show the isoscalar F_2 structure function computed with the SRC component, f_i^{SRC}, of the baseSRC PDFs divided by the aforementioned isoscalar combination. Both F_2^A and F_2 are calculated using the LO formula [69] at $Q = 10$ GeV. The baseSRC curve illustrates the shape of the relative nuclear modification, which is universal and independent of A. This nuclear modification is weighted by the SRC coefficients (typically ∼10% to 30%) and added to the proton PDF to yield the full nPDF.

and TRADITIONAL enhancements. Furthermore, at high-x value, above ∼0.6, the difference is most pronounced. Part of this enhanced high-x effect can be understood to result from the effects of Fermi motion that are known to grow with x and are included in our approach inside the modification function and therefore leads to the appearance of enhanced modification effects at high x [70].

As noted earlier, when we combine the elements of Fig. 2 to construct the nPDFs, we find that the valence nPDFs for the TRADITIONAL and SRC fits are identical, within uncertainties. This highlights the fact that the nPDFs are truly constrained by the data, despite the differing parametrizations.

Conclusions—We have performed the first-ever global QCD analysis of nuclear PDFs using a framework based on concepts from SRC nuclear models. It leads to similar, or better, data description as compared to the TRADITIONAL parametrization, and enables a meaningful physical interpretation of the fit. The incorporated data include the high-energy DIS, DY, and electroweak boson production commonly used in nPDF fits. The analysis determines both the standard "average" nuclear PDFs (that can be compared with TRADITIONAL nPDF fits), as well as a universal distribution of partons in SRC nucleon pairs and the fractions of such SRC pairs.

This analysis represents a direct extraction of nuclear structure information from experimental observables directly probing quark-gluon nuclei dynamics. The fact that the obtained fractions of SRC pairs agree with their previous extractions from the low-energy quasielastic data establishes a direct link between high-energy partonic properties and lower-energy nuclear physics. It thus presents a significant advance in our quest to understand atomic nuclei in terms of QCD. Furthermore, the extracted distributions of partons in SRC pairs can be directly tested using measurements of tagged processes at the Jefferson Lab accelerator and the future Electron-Ion Collider.

This new nPDF set can also potentially impact the analysis of heavy-ion measurements that require a combination of nuclear PDFs, together with initial state nuclear matter effects [71–73]. Whereas TRADITIONAL approaches thus far assign the same nPDF to all nucleons in the calculated initial-state distributions, the SRC approach allows additional flexibility. With the SRC PDFs, we can (i) follow the TRADITIONAL approach and simply use averaged distributions, or (ii) we can construct a more complex initial-state nucleon distribution using a combination of the free-nucleon PDF and SRC-modified PDF to each nucleon depending on its correlation state. Furthermore, it is noteworthy that the SRC parametrization (in which the dependence of A and x is factorized) produces an excellent description of the data; the conceptual simplicity of this parametrization is striking.

Acknowledgments—We are grateful to Jeff Owens and Efrain Segarra for valuable discussion. The work at University of Münster was funded by the DFG through the Research Training Group 2149 "Strong and Weak Interactions–from Hadrons to Dark Matter" and the SFB 1225 "Isoquant," project-id 273811115. The research of P. D. was funded as a part of the Center of Excellence in Quark Matter of the Academy of Finland (project 346326). M. K. thanks the School of Physics at the University of New South Wales in Sydney, Australia for its hospitality and financial support through the Gordon Godfrey visitors program. A. K. and N. D. are grateful for the support of Narodowe Centrum Nauki under grant no. 2019/34/E/ST2/00186. The work of C. K. was supported by the U.S. DOE contract DE-AC05-06OR23177, under which Jefferson Science Associates LLC manages and operates Jefferson Lab. J. G. M. has been supported by Fermi Research Alliance, LLC under Contract No. DE-AC02-07CH11359 with the U.S. DOE. F. O. was supported by the U.S. DOE under Grant No. DE-SC0010129, and the DOE Nuclear Physics, within the Saturated Glue (SURGE) Topical Theory Collaboration. R. R. is supported by the Polska Akademia Nauk (grant agreement PAN.BFD. S.BDN. 613.022.2021-PASIFIC 1, POPSICLE) and by Narodowe Centrum Nauki under Grant No. 2023/49/B/ST2/04330. This work has received funding from the European Union's Horizon 2020 research and innovation program under the Skłodowska-Curie grant agreement No. 847639 and from the Polish Ministry of Education and Science. The work of I. S. was supported by the French CNRS via the IN2P3 project GLUE@NLO. The work of E. P. was supported by the OPRA Association, Pazy foundation, and the Israeli Science Foundation (Grant 917/20).

[1] R. Abdul Khalek *et al.*, Nucl. Phys. **A1026**, 122447 (2022).
[2] J. C. Collins and D. E. Soper, Annu. Rev. Nucl. Part. Sci. **37**, 383 (1987).
[3] J. C. Collins, Phys. Rev. D **58**, 094002 (1998).
[4] J. Collins, *Foundations of Perturbative QCD* (Cambridge University Press, Cambridge, England, 2013), Vol. 32.
[5] S. Bailey, T. Cridge, L. A. Harland-Lang, A. D. Martin, and R. S. Thorne, Eur. Phys. J. C **81**, 341 (2021).
[6] R. D. Ball *et al.* (NNPDF Collaboration), Eur. Phys. J. C **82**, 428 (2022).
[7] T.-J. Hou *et al.*, Phys. Rev. D **103**, 014013 (2021).
[8] K. Kovarik *et al.*, Phys. Rev. D **93**, 085037 (2016).
[9] K. J. Eskola, P. Paakkinen, H. Paukkunen, and C. A. Salgado, Eur. Phys. J. C **82**, 413 (2022).
[10] I. Helenius, M. Walt, and W. Vogelsang, Phys. Rev. D **105**, 094031 (2022).
[11] R. Abdul Khalek, R. Gauld, T. Giani, E. R. Nocera, T. R. Rabemananjara, and J. Rojo, Eur. Phys. J. C **82**, 507 (2022).
[12] E. P. Segarra *et al.*, Phys. Rev. D **103**, 114015 (2021).
[13] R. Ruiz *et al.*, Prog. Part. Nucl. Phys. **136**, 104096 (2024).
[14] M. Alvioli, C. Ciofi degli Atti, B. Z. Kopeliovich, I. K. Potashnikova, and I. Schmidt, Phys. Rev. C **81**, 025204 (2010).
[15] B. Z. Kopeliovich, J. G. Morfin, and I. Schmidt, Prog. Part. Nucl. Phys. **68**, 314 (2013).
[16] A. Kusina *et al.*, Eur. Phys. J. C **80**, 968 (2020).
[17] P. Duwentäster, L. A. Husová, T. Ježo, M. Klasen, K. Kovařk, A. Kusina, K. F. Muzakka, F. I. Olness, I. Schienbein, and J. Y. Yu, Phys. Rev. D **104**, 094005 (2021).
[18] P. Duwentäster, T. Ježo, M. Klasen, K. Kovařík, A. Kusina, K. F. Muzakka, F. I. Olness, R. Ruiz, I. Schienbein, and J. Y. Yu, Phys. Rev. D **105**, 114043 (2022).
[19] K. F. Muzakka *et al.*, Phys. Rev. D **106**, 074004 (2022).
[20] K. J. Eskola, P. Paakkinen, H. Paukkunen, and C. A. Salgado, Eur. Phys. J. C **77**, 163 (2017).
[21] R. Abdul Khalek, J. J. Ethier, and J. Rojo (NNPDF Collaboration), Eur. Phys. J. C **79**, 471 (2019).
[22] R. Abdul Khalek, J. J. Ethier, J. Rojo, and G. van Weelden, J. High Energy Phys. 09 (2020) 183.
[23] M. Walt, I. Helenius, and W. Vogelsang, Phys. Rev. D **100**, 096015 (2019).
[24] D. de Florian, R. Sassot, P. Zurita, and M. Stratmann, Phys. Rev. D **85**, 074028 (2012).
[25] H. Khanpour and S. Atashbar Tehrani, Phys. Rev. D **93**, 014026 (2016).
[26] H. Khanpour, M. Soleymaninia, S. A. Tehrani, H. Spiesberger, and V. Guzey, Phys. Rev. D **104**, 034010 (2021).
[27] E. Caurier, G. Martinez-Pinedo, F. Nowacki, A. Poves, and A. P. Zuker, Rev. Mod. Phys. **77**, 427 (2005).
[28] R. Subedi *et al.*, Science **320**, 1476 (2008).
[29] O. Hen, G. A. Miller, E. Piasetzky, and L. B. Weinstein, Rev. Mod. Phys. **89**, 045002 (2017).
[30] C. Ciofi degli Atti, Phys. Rep. **590**, 1 (2015).
[31] C. Ciofi Degli Atti and S. Liuti, Phys. Lett. B **225**, 215 (1989).
[32] E. Piasetzky, M. Sargsian, L. Frankfurt, M. Strikman, and J. W. Watson, Phys. Rev. Lett. **97**, 162504 (2006).
[33] I. Korover *et al.* (Lab Hall A Collaboration), Phys. Rev. Lett. **113**, 022501 (2014).
[34] O. Hen *et al.*, Science **346**, 614 (2014).
[35] M. Duer *et al.* (CLAS Collaboration), Phys. Rev. Lett. **122**, 172502 (2019).
[36] I. Korover *et al.* (CLAS Collaboration), Phys. Lett. B **820**, 136523 (2021).
[37] J. R. West, Nucl. Phys. **A1029**, 122563 (2023).
[38] E. O. Cohen *et al.* (CLAS Collaboration), Phys. Rev. Lett. **121**, 092501 (2018).
[39] A. Schmidt *et al.* (CLAS Collaboration), Nature (London) **578**, 540 (2020).
[40] C. Ciofi degli Atti and H. Morita, Phys. Rev. C **96**, 064317 (2017).
[41] R. Weiss, I. Korover, E. Piasetzky, O. Hen, and N. Barnea, Phys. Lett. B **791**, 242 (2019).
[42] C. Ciofi degli Atti and S. Simula, Phys. Rev. C **53**, 1689 (1996).
[43] J. R. Pybus, I. Korover, R. Weiss, A. Schmidt, N. Barnea, D. W. Higinbotham, E. Piasetzky, M. Strikman, L. B. Weinstein, and O. Hen, Phys. Lett. B **805**, 135429 (2020).
[44] R. Weiss, B. Bazak, and N. Barnea, Phys. Rev. C **92**, 054311 (2015).
[45] R. Weiss, R. Cruz-Torres, N. Barnea, E. Piasetzky, and O. Hen, Phys. Lett. B **780**, 211 (2018).
[46] R. Cruz-Torres, D. Lonardoni, R. Weiss, N. Barnea, D. W. Higinbotham, E. Piasetzky, A. Schmidt, L. B. Weinstein, R. B. Wiringa, and O. Hen, Nat. Phys. **17**, 306 (2021).
[47] J. C. Collins, D. E. Soper, and G. F. Sterman, Nucl. Phys. **B261**, 104 (1985).
[48] K. S. Egiyan *et al.* (CLAS Collaboration), Phys. Rev. Lett. **96**, 082501 (2006).
[49] N. Fomin *et al.*, Phys. Rev. Lett. **108**, 092502 (2012).
[50] B. Schmookler *et al.* (CLAS Collaboration), Nature (London) **566**, 354 (2019).
[51] L. B. Weinstein, E. Piasetzky, D. W. Higinbotham, J. Gomez, O. Hen, and R. Shneor, Phys. Rev. Lett. **106**, 052301 (2011).
[52] O. Hen, E. Piasetzky, and L. B. Weinstein, Phys. Rev. C **85**, 047301 (2012).
[53] O. Hen, D. W. Higinbotham, G. A. Miller, E. Piasetzky, and L. B. Weinstein, Int. J. Mod. Phys. E **22**, 1330017 (2013).
[54] E. P. Segarra, A. Schmidt, T. Kutz, D. W. Higinbotham, E. Piasetzky, M. Strikman, L. B. Weinstein, and O. Hen, Phys. Rev. Lett. **124**, 092002 (2020).
[55] G. A. Miller and J. E. Spencer, Ann. Phys. (N.Y.) **100**, 562 (1976).
[56] R. Cruz-Torres, A. Schmidt, G. A. Miller, L. B. Weinstein, N. Barnea, R. Weiss, E. Piasetzky, and O. Hen, Phys. Lett. B **785**, 304 (2018).
[57] See Supplemental Material at http://link.aps.org/supplemental/10.1103/PhysRevLett.133.152502 for further information on the data and the fit methodology, which includes Refs. [58–65].
[58] H. Abramowicz *et al.* (H1, ZEUS Collaborations), Eur. Phys. J. C **75**, 580 (2015).
[59] A. Accardi, L. T. Brady, W. Melnitchouk, J. F. Owens, and N. Sato, Phys. Rev. D **93**, 114017 (2016).
[60] R. D. Ball *et al.* (NNPDF Collaboration), Eur. Phys. J. C **77**, 663 (2017).
[61] G. P. Salam and J. Rojo, Comput. Phys. Commun. **180**, 120 (2009).

[62] T. Carli, D. Clements, A. Cooper-Sarkar, C. Gwenlan, G. P. Salam, F. Siegert, P. Starovoitov, and M. Sutton, Eur. Phys. J. C **66**, 503 (2010).
[63] J. M. Campbell, R. K. Ellis, and W. T. Giele, Eur. Phys. J. C **75**, 246 (2015).
[64] Y. Li and F. Petriello, Phys. Rev. D **86**, 094034 (2012).
[65] S. Alekhin *et al.*, Eur. Phys. J. C **75**, 304 (2015).
[66] D. Stump, J. Huston, J. Pumplin, W.-K. Tung, H. L. Lai, S. Kuhlmann, and J. F. Owens, J. High Energy Phys. 10 (2003) 046.
[67] K. A. Griffioen *et al.*, Phys. Rev. C **92**, 015211 (2015).
[68] S. Li *et al.*, Nature (London) **609**, 41 (2022).
[69] P. A. Zyla *et al.* (Particle Data Group), Prog. Theor. Exp. Phys. **2020**, 083C01 (2020).
[70] E. P. Segarra, J. R. Pybus, F. Hauenstein, D. W. Higinbotham, G. A. Miller, E. Piasetzky, A. Schmidt, M. Strikman, L. B. Weinstein, and O. Hen, Phys. Rev. Res. **3**, 023240 (2021).
[71] E. G. Ferreiro, F. Fleuret, J. P. Lansberg, and A. Rakotozafindrabe, Phys. Lett. B **680**, 50 (2009).
[72] E. G. Ferreiro, F. Fleuret, J. P. Lansberg, and A. Rakotozafindrabe, Phys. Rev. C **81**, 064911 (2010).
[73] E. G. Ferreiro, F. Fleuret, J. P. Lansberg, N. Matagne, and A. Rakotozafindrabe, Few Body Syst. **53**, 27 (2012).